

## ABSTRACT

This article presents the identification process of high temperatures in low voltage (LV) turrets of a single-phase generator step-up (GSU) transformer which is equipped with non-magnetic stainless steel (SS) inserts in the turrets. High temperatures are detected in the SS insert regions of the LV turrets utilizing thermography cameras and temperature labels. The presence of high temperature in the LV turrets generated issues in the transformer as the crystallization of the turret gasket seals and the presence of transformer oil leaks. To figure out the cause of the high temperature in the turrets, three-dimensional (3-D) finite element (FE) simulations are performed. Electromagnetic analyses coupled with thermal analyses are carried out to understand the origin of the high temperatures in the turrets of the GSU transformer. To validate the 3-D FE transformer model, the results of the FE simulations are compared with the temperature measurements in the turrets. With the FE simulation results, the author detected magnetic design issues related to the SS inserts and related to the magnetic material utilized in the turrets, which are producing high temperatures. The study presented could help transformer manufacturers to predict and prevent possible heating issues in GSU transformers in the LV turret regions.



## KEYWORDS:

generator step-up (GSU) transformer, low voltage (LV) turret, finite element (FE), stray loss, infrared thermography, stainless steel insert, hot spot temperature, current transformer (CT)

**Timely identification of high-temperature issues in generator step-up transformers is a fundamental preventive process to avoid catastrophic failures that could have devastating consequences**

# Detection and reduction of high temperature in high current turrets of generator step-up (GSU) transformers – Part I

## 1. Introduction

Timely identification of high-temperature issues in generator step-up (GSU) transformers is a fundamental preventive process to avoid catastrophic failures that could have devastating consequences for the process of generation of electrical energy in power stations [1], [2]. In GSU transformers, one of the causes of failure is related to overheating and the presence of high temperatures in bushing regions and tanks [3], [4]. Transformer standards specify that temperatures between 95 and 105 °C are permissible in bushing turrets where rated continuous currents exceed 5 kA [5], [6]. The temperature in turrets should be kept in this temperature range to avoid possible damage to the gasket seals and the presence of transformer oil leaks [7]. Some methodologies to identify and reduce high temperatures in low voltage (LV) turrets of GSU transformers have been studied and published. For example, in [8], the authors presented a methodology to identify hot spots in GSU transformers. This methodology is based on the detection of dissolved gases and thermography tests. Employing temperature measurements, analytical formulations, and three-dimensional (3-D) FE simulations, the authors found hot spots in the low carbon steel structural supports for current transformers (CTs) which are in the interior of the LV turrets and closed to the LV bushing conductors. Low carbon steel CT supports and the turret regions presented temperatures above 140 °C (hot spot temperature). The authors replaced the low carbon steel CT supports with non-magnetic stainless steel (SS) CT supports to eliminate the presence of hot spots in the turrets. With the SS CT supports, the GSU transformer presented temperatures around 100 °C in the turrets. In [9], the author utilized thermography cameras to detect hot spots in the LV turrets of a three-phase GSU transformer. To reduce the temperature in the turrets, the author decided to use SS inserts and SS shorting plates. A set of SS inserts were made in the turrets, and some SS shorting plates were welded to the surface of the inserts. The shorting plates of each turret

**3-D FE simulations have been performed to understand the main cause of the presence of high temperature in the turrets of this GSU transformer**

were welded between them to produce a closed path for the eddy currents induced in each turret. The eddy currents circulate from one turret to another turret using the shorting plates, reducing the power losses and temperature in the turrets. This technique works well, and the temperature of the turrets was reduced successfully.

The main contribution of this article is the identification of high temperatures in LV turrets of a real GSU transformer equipped with SS inserts. It is demonstrates that the presence of these SS inserts and the magnetic material utilized in the turrets produce high temperatures in the GSU transformer. 3-D FE simulations have been performed to understand the main cause of the presence of high temperature in the turrets of this GSU transformer.

*The solution for this GSU transformer heating issue will be presented by the author in the next "Transformers Magazine" edition.*

Table 1. Characteristics of GSU transformer

| Nominal transformer rating | 90 MVA |
|---|---|
| Impedance | 13.7 % |
| Phases | 1 |
| Nominal low voltage (LV) current | 6.82 kA |
| Nominal high voltage (HV) current | 678 A |
| Cooling system | FOW |
| Year of manufacturing | 1991 |
| Primary and secondary voltage | 13.2/230 kV |
| Frequency | 60 Hz |

Figure 1. Photo of 90 MVA single-phase GSU transformer

## 2. Identification of high temperature in turrets of GSU transformer

The background and identification process of the high temperatures in the LV turrets of a single-phase GSU transformer are presented in this section. The GSU transformer analyzed in this article is operating in Unit 2 in the "El Guavio" hydroelectric power station in Colombia [10].

### 2.1 Characteristics of GSU power transformer

Table 1 shows the technical characteristics of the 90 MVA single-phase GSU transformer under study. Fig. 1 shows a photo of the 90 MVA single-phase GSU transformer under normal operation. The LV turrets of this transformer were originally manufactured of low carbon steel. In addition, this GSU transformer has a couple of non-magnetic SS inserts in the LV turrets. The SS inserts were done by the transformer manufacturer to reduce stray losses and temperature in the turrets. Fig. 2 shows the non-magnetic SS inserts located in the LV turrets of the real GSU transformer. Generally, non-magnetic SS inserts are utilized to reduce stray losses in the tank regions of power transformers where high current bushings are present [11]. The correct use of the SS inserts helps to reduce in more than 80 % the stray losses in tank regions of power transformers [11].

### 2.2. Temperature measurements

Transformer oil leaks were detected in the GSU transformer in the regions of the LV turrets. Power station personal detected the oil leaks, and they decided to analyze the state of the gasket seals in the LV turrets regions. The gasket seals were found crystallized, which generated the oil leaks in the GSU transformer. The presence of crystallized gasket seals was an indication of the presence of high

**Non-magnetic SS inserts are utilized to reduce stray losses in the tank regions of power transformers**

temperatures in the turrets. No dissolved gases we detected in the GSU transformer during this time. As part of preventive maintenance, the power station personal decided to monitor the temperature of this transformer using infrared thermography cameras [12]. During this monitoring process, temperatures > 100 °C were measured in the LV turrets when the LV bushing conductors carried 95 % of the nominal current. Temperatures between 104 and 114 °C were detected in the regions of the turrets in the region above the SS inserts. Fig. 3 shows photos of the measured temperature in the turrets at 95 % of the nominal current. From the temperature measurements at 95 % of nominal current, power station personal decided to perform spot temperature measurements utilizing temperature labels to measure the temperature in the turret region above the SS inserts. The scale of the temperature labels is between 116 and 154 °C. These spot temperature tests were carried out at 100 % of the nominal current. Fig. 4 shows photos of the temperature values measured in the LV turrets at 100 % of the nominal current. Temperatures between 110 and 120 °C were measured in the turret region above the SS inserts.

**Temperatures over 100 °C were measured in the LV turrets when the LV bushing conductors carried 95 % of the nominal current**

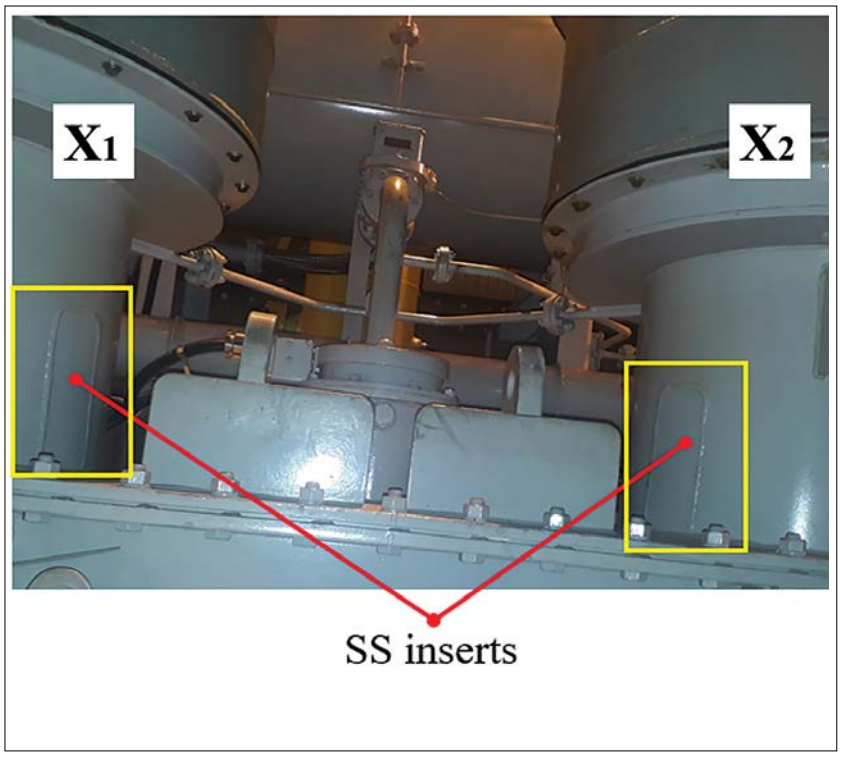


Figure 2. Stainless steel (SS) inserts in LV turrets

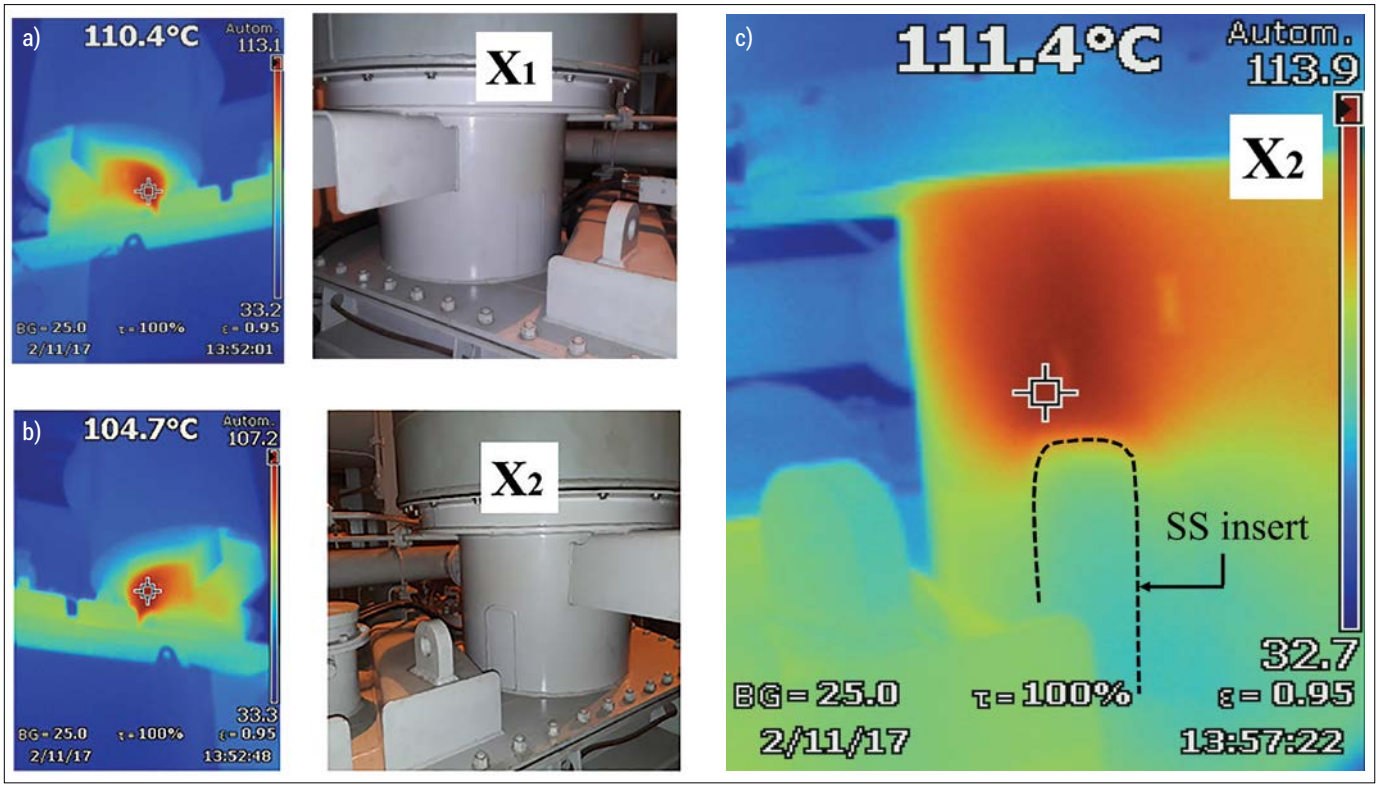


Figure 3. Temperatures measured in the LV turrets with SS inserts at 95 % of nominal current: a) LV turret $X_1$, b) LV turret $X_2$, c) detailed temperature distribution in the LV turret $X_2$


Figure 4. Temperatures measured in the LV turrets with SS inserts at 100 % of nominal current: a) LV turret $X_1$, b) LV turret $X_2$

**With the conducted measurements and visual inspections, it was clear that this GSU transformer has an issue with high temperatures in the LV turrets in the region above the SS inserts**

With the results of the temperature tests, the GSU transformer was taken out of service for a detailed inspection. A visual inspection was performed to verify the state of the LV bushing-turret regions of the GSU transformer. Some visible heating damage was detected in the internal region of the LV turrets in the region above the SS inserts. Fig. 5 shows a photo of the internal region of an LV turret with visible heating signs above the SS insert. With the conducted measurements and visual inspections, it was clear that this GSU transformer has an issue with high temperatures in the LV turrets in the region above the SS inserts. To figure out the origin or cause of the high temperature in the turrets, some 3-D FE simulations (electromagnetic and thermal analyses coupled) were performed. In Section 3, the process of the FE simulations and their validation are presented. The origin or causes of the presence of high temperatures in the turrets is explained utilizing the results obtained from the FE simulations.

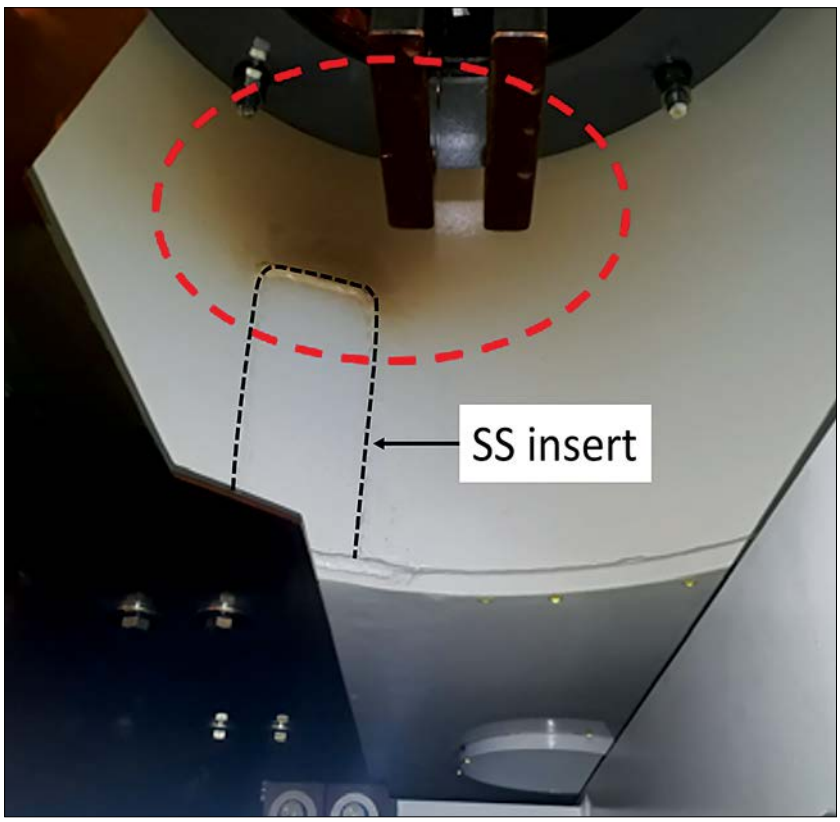


Figure 5. Photo of visible heating signs in the region above the SS insert

## 3. Finite element simulations

3-D FE simulations are performed to compute the stray losses and the distributions of temperature in the LV turrets of the 90 MVA single-phase GSU transformer. The stray losses in the turrets are computed by performing time-harmonic analyses. Performing static thermal analyses and utilizing the stray losses computed in the time-harmonic analysis as heat sources, the temperature distributions in the turrets are computed. More details about the finite element models and simulation process are briefly described in this section.

**3-D FE simulations are performed to compute the stray losses and the distributions of temperature in the LV turrets of the 90 MVA single-phase GSU transformer**

### 3.1 Characteristics of the turret model

Fig. 6 shows the 3-D model of the LV turret of the GSU transformer with the SS insert. The turret with the SS insert and the bushing conductor is considered in the model. The turret has an inner diameter of 594 mm, a height of 460 mm, and a thickness of 6.35 mm. The radius of the bushing conductor is 150 mm. The SS insert has a height $h_{ssi}$ = 230 mm, a width $w_{ssi}$ = 80 mm, and a thickness of 6.35 mm. The tank cover and other structural elements located on the tank cover were omitted in the FE analysis.

The LV turret is made of low carbon steel, which has a relative permeability $\mu_{rcs}$ = 200 and an electrical conductivity $\sigma_{cs} = 4 \times 10^6$ S/m, which corresponds to 120 °C [13]. The bushing conductor is made of copper with a relative permeability $\mu_r$ = 1 and a conductivity $\sigma_{cu} = 5.8 \times 10^7$ S/m. The SS insert has an electrical conductivity $\sigma_{ss} = 1.1 \times 10^6$ S/m and a relative permeability $\mu_r$ = 1.

A total of 500,000 tetrahedral FEs are employed in the LV turret model of the GSU transformer.

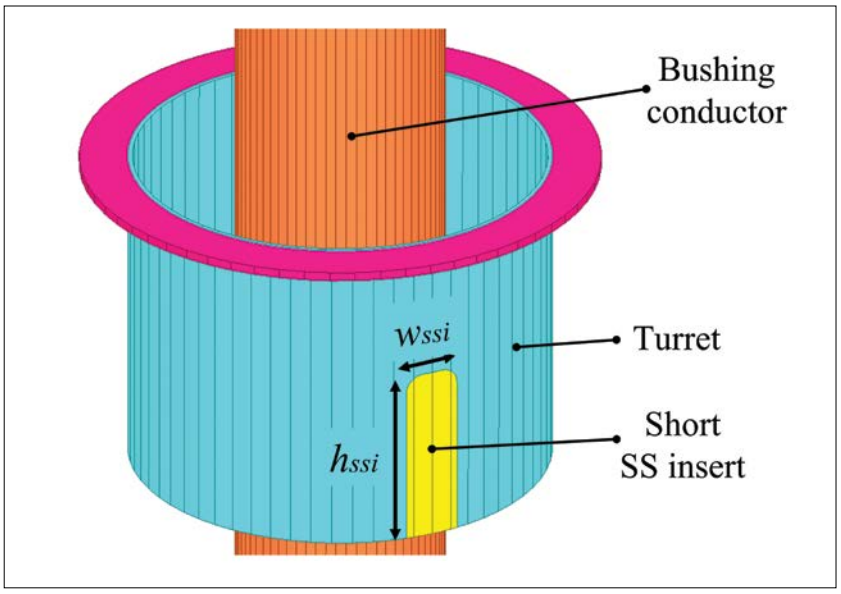

Figure 6. Model of LV turret with the SS insert

**Because of the computational complexity of the 3-D FE model to compute stray losses in thick low carbon steel turrets, surface impedance boundary conditions (SIBCs) are employed to compute the stray losses in the turrets of the GSU transformer**

### 3.2 Computation of stray losses in turret model

Because of the computational complexity of the 3-D FE model to compute stray losses in thick low carbon steel turrets, surface impedance boundary conditions (SIBCs) are employed to compute the stray losses in the turrets of the GSU transformer [14]. The SIBCs are utilized to compute the stray losses in the turrets which have a greater plate thickness (6.35 mm) compared with the skin depth of the low carbon steel at f = 60 Hz ($\delta_{cs}$ = 2.29 mm). One can see in Fig. 6 that the cylindrical turret structure is modeled as a polyhedron. The SIBCs are applied only in flat faces where stray losses need to be computed. For this reason, the cylindrical turret structure needs to be modeled as a polyhedron to apply the SIBCs in each face of the polyhedron. In addition, the use of polyhedrons in the cylindrical turret structure and the bushing conductor helps to facilitate the adaptation of the finite element mesh during the adaptive meshing process reducing the computation times.

Moreover, the skin depth of the non-magnetic stainless steel at f = 60 Hz ($\boldsymbol{\delta}_{ss}$ = 61.95 mm) is greater than the insert thickness (6.35 mm). For this reason, it is not necessary to employ SIBCs in the SS insert. In the SS insert is necessary only to apply a normal but adequate finite element mesh to compute the stray losses.

### 3.3 Multiphysics finite element analysis

A Multiphysics finite element analysis is performed to compute the distribution of temperature in the LV turret. The stray losses computed in the electromagnetic analysis are coupled with the static thermal analysis to compute the distribution of temperature in the LV turret model. Thermal properties have been assigned to the LV turret, and SS insert. The low carbon steel of the turret has a thermal conductivity of 60.5 W/m °C, and the non-magnetic stainless steel has a thermal conductivity of 15.1 W/m °C. A convection coefficient h = 5 W/m$^2$ °C at 30 °C is utilized in the external surfaces of the SS insert and LV turret to simulate the natural convection between the LV turret and the SS insert with the surrounding air. Another convection coefficient h = 58 W/m$^2$°C at 65 °C is utilized in the internal surfaces of the LV turret, and SS insert to simulate the forced convection between the surrounding transformer oil and the internal surfaces of the LV turret and SS insert.

**The stray losses computed in the electromagnetic analysis are coupled with the static thermal analysis to compute the distribution of temperature in the LV turret model**

**A stray loss of 2.26 kW is computed in the turret, and a stray loss of 17 mW is calculated in the SS insert**

### 3.4 Preliminary static magnetic field analysis

Preliminary magnetostatic analyses are performed to compute the magnetic field distribution in the LV turret with the SS insert applying 100 % of the nominal current $I_{nom}$ = 6.82 kA in the bushing conductor. Fig. 7 shows the flux density distribution in the turret with the SS insert, and Fig. 8 shows a detailed view of the vector field distribution of flux density in the turret region above the SS insert. In Figs. 7 and 8, one can see high values of flux densities in the turret region above the SS insert. A maximum flux density of 1.91 T is computed in this region above the SS insert. The SS insert can be seen as a region with a high reluctance compared with the reluctance presented by the whole region of the turret, including the turret region above the SS insert. In this case, the cross-section of the turret above the SS insert is 50 % less than the cross-section of the turret. Under these circumstances, the magnetic field circulating in the turret prefers to go above the SS insert, where the accumulation of magnetic flux produces high flux densities. The high flux density should produce considerable power losses in the turret zone above the SS insert. To deduce if the presence of the SS insert is the cause of the presence of high temperature in the turret, 3-D FE time-harmonic analysis coupled with 3-D FE static thermal analysis should be performed to compute the stray loss and temperature in the LV turret with the SS insert.

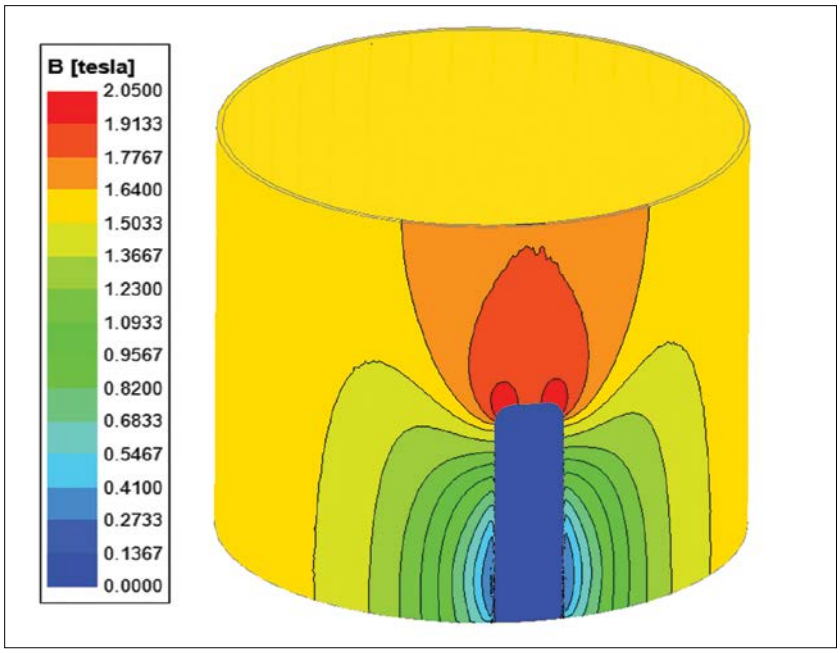


Figure 7. Magnetic flux density distribution in the turret with the SS insert.

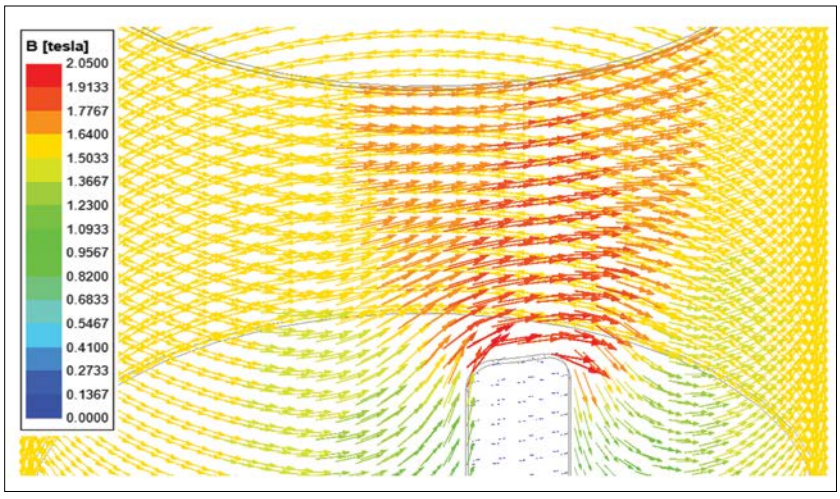


Figure 8. Detailed view of the magnetic flux density distribution in the region above the SS insert region.

### 3.5 Validation of the turret model

The 3-D model of the LV turret with the SS insert is analyzed and validated by performing a 3-D electromagnetic FE simulation applying $I_{nom}$ = 6.82 kA at 60 Hz in the bushing conductor. Fig. 9 shows the loss distribution in the turret with the SS insert. A stray loss $P_{cs}$ = 2.26 kW is computed in the turret, and a stray loss $P_{ss}$ = 17 mW is calculated in the SS insert. One can see high stray losses in the region above the SS insert, where a high flux density is produced by the presence of the SS insert, see Figs. 7 and 8. This high flux density produces high losses in the region above the SS insert compared with the losses in the whole region of the turret.

Fig. 10 shows the temperature distribution in the LV turret with the SS insert. One can note from Fig. 10 that the presence of the SS insert produces a high-temperature region in the turret in the zone above the SS insert. A maximum temperature of 120.61 °C is computed in the zone above the SS insert.

In addition, a 3-D FE simulation is performed to compute the temperature in the turret without the SS insert using the same electromagnetic and thermal conditions utilized in the Multiphysics analysis for the turret with the SS insert. Table 2 shows the maximum temperature values computed in the FE simulation for the turret with and without a SS insert. The turret with the SS insert presented a high temperature compared with the turret without the SS insert. A maximum difference of 10.85 °C is calculated between the turret with the SS insert and the turret without the SS insert. Furthermore, the temperature computed in the turret (see Fig. 10) with the SS insert shows a good

agreement with the temperature measured in the turret with the SS insert (see Fig. 4). Table 3 shows the results of maximum temperature computed and measured in the region above the SS insert in the turret for 100 % and 95 % of $I_{nom}$. Differences of less than 1 °C are calculated between the temperature calculated in the FE simulations and the temperature measured in the turrets of the GSU transformer. The FE model of the turret is validated with the results presented in Tables 2 and 3.

Finally, the author concluded that the presence of high temperatures ($T_{max}$ > 105 °C) in the LV turrets is produced for the use of low carbon steel in the turret structure and by the presence of the SS inserts. Both factors contribute to the presence of high temperature in the LV turrets of the GSU transformer. A flexible and economical magnetic solution needs to be proposed to reduce the temperature in the LV turrets utilizing the actual turret structure of the GSU transformer.

## 4. Conclusion

High temperatures and transformer oil leaks were detected in the LV turrets of a GSU transformer. The high temperatures in the LV turrets were detected utilizing thermography cameras and

**It was concluded that the presence of high temperatures ($T_{max}$ > 105 °C) in the LV turrets is produced for the use of low carbon steel in the turret structure and by the presence of the SS inserts**

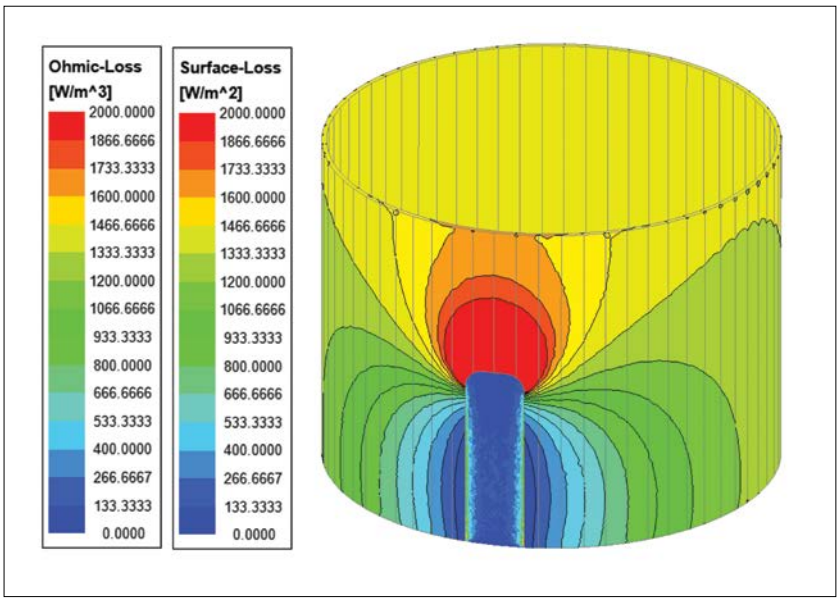


Figure 9. Loss density distribution (in W/m²) in the turret and power loss distribution (in W/m³) in the SS insert.

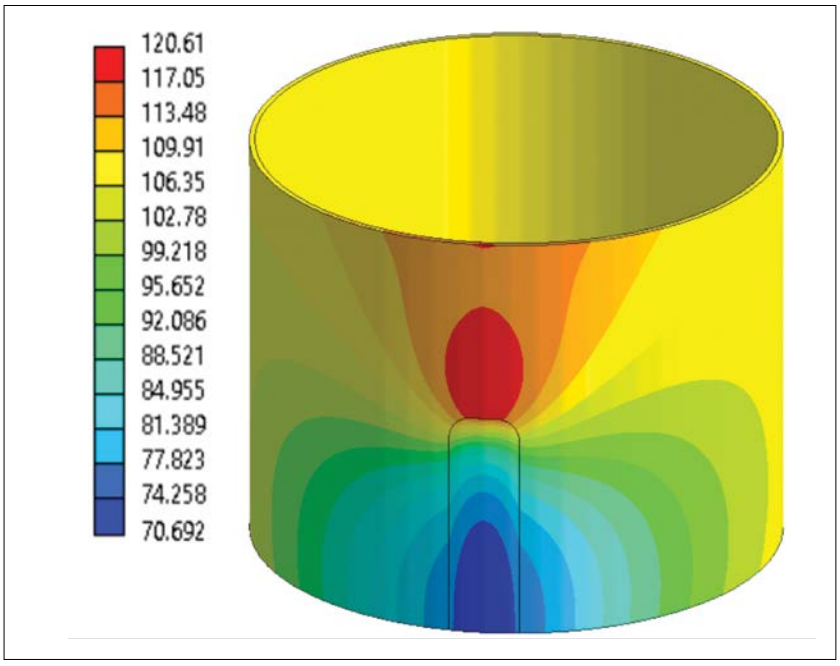


Figure 10. Temperature distribution (in °C) in the turret with the SS insert.

Table 2. Maximum temperature computed in the LV turret with and without SS insert

| Case | Temperature (FE simulation) |
|---|---|
| **LV turret without SS insert** | 109.76 °C |
| **LV turret with SS insert** | 120.61 °C |

Table 3. Maximum temperature measured and computed in the turret region above the SS insert for different currents in the bushing conductor

| Bushing current | Temperature (°C) (Measured) | Temperature (°C) (FE simulation) | Difference (°C) |
|---|---|---|---|
| 6.82 kA | 120 | 120.61 | 0.61 |
| 6.48 kA | 114 | 114.93 | 0.93 |

temperature labels. The causes of the high temperatures in the LV turrets were investigated and analyzed. It was demonstrated that the high temperature in the LV turrets is produced by the low carbon steel utilized in the turrets and by the presence of the SS inserts. Performing 3-D FE simulations, the author demonstrated that the presence of the SS inserts produces a region of high stray losses, which produces high temperatures in the turrets. The results obtained in the FE simulations are compared and validated with the real temperature measurements. Differences of less than 1 % are obtained between the FE simulations and the temperature measurements.

To mitigate the temperature in the turrets, a magnetic solution will be proposed without replacing the original carbon steel turrets with new turrets manufactured completely of stainless steel.

***The magnetic solution will be presented in the next edition of "Transformers Magazine".***

## Acknowledgments

The author would like to thank Luis A. Garcia from Enel-Emgesa and the staff of the "El Guavio" hydroelectric power station for the technical information and temperature measurements.

## Bibliography

[1] X. Dong et al., *Study of abnormal electrical phenomena effects on GSU transformers*," *IEEE Trans. Power Delivery*, vol. 18, no. 3, pp. 835–842, 2003

[2] B. M. Pasternack, J. H. Provanzana, L. B. Wagenar, *Analysis of a generator step-up transformer failure following faulty synchronization*, *IEEE Trans. Power Delivery*, vol. 3, no. 3, pp. 1051–1058, 1988

[3] T. Lin, *Transformer bushing monitoring*, Transformers Magazine, Special Edition: Bushings, pp. 108- 115, November 2017

[4] R. Actis, R. Maina, V. Tumiatti, *Diagnostics of HV bushings through oil sampling and analysis*, Transformers Magazine, Special Edition: Bushings, pp. 142–147, November 2017

*[5] IEEE standard for performance characteristics and dimensions for high current power transformer bushings with rated continuous current in excess of 5000 A in bus enclosures*, IEEE Std C57.19.04-2018, pp. 1–24, June 2018

[6] M. Akbari, M. Allahbakhshi, R. Mahmoodian, *Heat analysis of the power transformer bushings in the transient and steady states considering the load variations*, Applied Thermal Engineering, vol. 121, pp. 999-1010, 2017

[7] S. H. Wickman, *Transformer bushings and oil leaks*, Transformers Magazine, Special Edition: Bushings, pp. 148–154, November 2017

[8] A. de Souza Melo et al., *Identifying hot spots in GSU power transformers using multiple methods*, IET Science, Measurement & Technology, 2020, vol. 14, no. 2, pp. 233–240, 2020

*[9] Persistence leads to hot-spot solution*, ReliablePlant Magazine, no. 5, September–October 2007, [Online] available: https://www.reliableplant.com/Read/7947/persistence-hot-spot-solution [accessed: September 2021]

[10] V. Martínez, O. L. Castillo, *The political ecology of hydropower: Social justice and conflict in Colombian hydroelectricity development*, Energy Research & Social Science, vol. 22, pp. 69–78, 2016

[11] S. Magdaleno-Adame et al., *Reduction of stray losses in tertiary voltage bushings in power transformer tanks*, *2014 IEEE International Autumn Meeting on Power, Electronics and Computing*, pp. 1–5, 2014

[12] R. Thompson, *Adaptive response technology*, Transformers Magazine, Special Edition: Bushings, pp. 82–87, November 2017

[13] A. N. Bhagat, S. Ranganathan, O. N. Mohanty, *Electrical resistivity studies in low carbon and HSLA-100 steels*, Materials Science and Technology, vol. 19, no. 3, pp. 343–346, 2003

[14] R. M. Del Vecchio et al., Transformer Design Principles, Third Edition, CRC Press: Boca Raton, FL, USA, 2017

## Author

**Salvador Magdaleno-Adame** was born in La Piedad de Cabadas, Michoacan, Mexico, in 1983. He received the B.Sc. degree in electrical engineering from the Universidad Michoacana de San Nicolas de Hidalgo, Morelia, Mexico, in 2008, and the M.Sc. degree in electrical engineering from the Instituto Tecnologico de Morelia, Morelia, in 2013. From 2008 until 2010 he worked at Industrias IEM S.A. de C.V. in Mexico as an R&D engineer in the technology department for power transformers where he conducted research on shell-type and core-type power transformers, and he also worked on the development of HV shunt reactors. He has occupied several magnetic engineering positions in companies in the USA, working in different magnetic and electromagnetic technologies, including transformers, motors, magnetic actuators, loudspeakers, permanent magnet technologies, magnetic materials, etc. He has authored over 60 papers. For many years, he has worked on a range of ideas and techniques to reduce the power losses in power transformers and distribution transformers. He owns a consultancy business called "Salvador Consultant – www.salvadorconsultant.com" to support the magnetic and electromagnetic industry in the USA. His current research interests include numerical calculation of electromagnetic fields in electromagnetic devices and transformers using the finite-element method, application of different magnetic materials in electromagnetic devices, design of magnetizing fixtures utilized in the magnetization process of permanent magnets, and the development of new magnetic technologies for different applications and industries.